ELSEVIER

International Journal of Applied Earth Observation and Geoinformation 10 (2008) 330–341

INTERNATIONAL JOURNAL OF APPLIED EARTH OBSERVATION AND GEOINFORMATION

www.elsevier.com/locate/jag

Approaches for comparative evaluation of raster GIS-based landslide susceptibility zonation maps

R.P. Gupta [a], D.P. Kanungo [b,*], M.K. Arora [c], S. Sarkar [b]

[a] *Department of Earth Sciences, Indian Institute of Technology Roorkee, Roorkee 247667, India*
[b] *Geotechnical Engineering Division, Central Building Research Institute, Roorkee 247667, India*
[c] *Department of Civil Engineering, Indian Institute of Technology Roorkee, Roorkee 247667, India*

Received 16 February 2007; accepted 22 January 2008

Abstract

Evaluation of maps generated from different conceptual models or data processing approaches at spatial level has importance in many geoenvironmental applications. This paper addresses the spatial comparison of different landslide susceptibility zonation (LSZ) raster maps of the same area derived from various procedures.

In hilly regions such as the Himalayas, occurrence of landslides is frequent, which necessitates the study of landslides in the region for future developmental planning. A critical aspect in landslide studies is the procedure for assignment of weights to various causative factors affecting the occurrence of landslides. A detailed study on conventional, artificial neural network (ANN) black box, fuzzy set based and combined neural and fuzzy weighting procedures for LSZ mapping in the Himalayas has recently been published by the authors in [Kanungo, D.P., Arora, M.K., Sarkar, S., Gupta, R.P., 2006. A comparative study of conventional, ANN black box, fuzzy and combined neural and fuzzy weighting procedures for landslide susceptibility zonation in Darjeeling Himalayas. Engineering Geology 85, 347–366]. The evaluation of various maps in that study was however based only on comparison of areal extents of various landslide susceptibility zones. In this paper, we present a spatial level comparative evaluation of those maps to get a detailed insight into the performance of each of the weighting procedures for landslide susceptibility zonation. The evaluation has been done through three approaches, viz., landslide density analysis, error matrix analysis and difference image analysis. Based on the landslide density values, it is inferred that the combined neural and fuzzy procedure for LSZ mapping appears to be significantly better than other procedures. The error matrix analysis highlights the significant difference between the conventional subjective weight assignment procedure and the objective combined neural and fuzzy procedure. Finally, the significant influence of a causative factor has been revealed by difference image analysis. The use of these spatial evaluation approaches in tandem may be highly beneficial to quantitatively assess the landslide susceptibility zonation or any other such maps.

Keywords: Landslide susceptibility zonation; Comparative evaluation; Density analysis; Error matrix analysis; Difference image analysis

1. Introduction

During the last 3–4 decades, the advent of satellite-sensor Remote Sensing and Geographical Information System (GIS) techniques has resulted in proliferation of spatial data and maps on global basis. The maps may possess different data structures (raster or vector), and may exhibit a variety of themes (e.g. land-use, lithology,

* Corresponding author. Tel.: +91 1332 283418; fax: +91 1332 272272.
E-mail addresses: rpgesfes@iitr.ernet.in (R.P. Gupta), debi.kanungo@gmail.com (D.P. Kanungo), manojfce@iitr.ernet.in (M.K. Arora), shantanu_cbri@yahoo.co.in (S. Sarkar).

0303-2434/$ – see front matter © 2008 Elsevier B.V. All rights reserved.
doi:10.1016/j.jag.2008.01.003

soil cover, depth to water table, etc.). At times there is a situation where several maps showing the same thematic attribute of the same area (e.g. vegetation density or landslide susceptibility) are available and exhibit differences due to different pre-processing approaches, presumptions, conceptual models, algorithms, or simply temporal factors. This necessitates the development of appropriate map comparison approaches and has created a growing interest among researchers over the years (e.g. Monserud and Leemans, 1992; Winter, 2000; Hagen, 2003; Pontius et al., 2004).

The GIS-based data analysis procedures provide ways and means to integrate diverse spatial data (e.g. Bonham-Carter, 1994; Carrara and Guzzetti, 1995; DeMers, 2000; Gupta, 2003). The advanced GIS computational tools offer numerous advantages in multi-geodata handling, as is evident from various geoenvironmental studies. However, these studies lack spatial level comparison of GIS derived maps. The focus of this paper is on comparative evaluation of spatial maps through different approaches.

Landslides and landslide susceptibility zonation (LSZ) studies have drawn considerable attention during the last few years. An LSZ map ranks areas or zones into different degree of existing or potential hazard of landslides. It typically shows spatial distribution of regions of different landslide susceptibilities, for example, zones pertaining to very high (VHS), high (HS), moderate (MS), low (LS) and very low (VLS) landslide susceptibility, which are rendered on an ordinal scale. Examples of many such maps produced from GIS-based approaches utilizing different weight assignment procedures have been published in the literature (e.g. Gupta and Joshi, 1990; Sarkar et al., 1995; Gupta et al., 1999; Sarkar and Kanungo, 2004; Saha et al., 2005; Kanungo et al., 2006).

The GIS-based LSZ maps are of both raster and vector types. Raster data operations have their own advantages as these can exhibit spatial variation effectively, affords ability to deduce variation in different image data at a point or in a local region (point and local image processing operations, see, e.g. Gonzalez and Woods, 2002; Gupta, 2003) and can also be displayed efficiently. Therefore, a raster data processing approach has been followed here. Moreover, the thematic data layers pertaining to various causative factors influencing the occurrence of landslides have been prepared from remote sensing data, for which the raster based processing in GIS environment was the automatic choice.

In this study, LSZ raster maps generated from four weight assignment procedures, namely, conventional subjective weight rating, ANN black box, fuzzy, and combined neural and fuzzy procedures (Kanungo et al., 2006) have been comparatively evaluated. This comparison will enable the understanding of differences in various procedures, and influence of various causative factors on occurrences of landslides in a test area in Darjeeling Himalayas.

2. Study area

The Darjeeling Himalayas, encompassing a total area of 3000 km^2 rise abruptly from the alluvial plains of West Bengal and attain a maximum elevation of about 2600 m. The study area encompasses Darjeeling hill which lies between latitude 26°56′N–27°8′N and longitude 88°10′E–88°25′E and covers an area of about 254 km^2 (Fig. 1). The main habitat areas are Darjeeling, Ghum, Sonada and Sukhiapokhri. The maximum elevation of 2584 m occurs at the Tiger hill. The area is dominated by mild slopes ranging between 15° and 35°, while steep slopes of >35° occupy small portion of the area. The annual rainfall in the area is of the order of 3000–6000 mm. The main land use practice in the study area is tea plantation and agriculture is mostly developed around the habitat areas.

3. Thematic data layers and LSZ mapping of the area—a brief description

LSZ maps of the area were prepared using four different approaches under the domain of remote sensing and GIS. These approaches are: (i) conventional subjective weighting approach, (ii) ANN black box approach, (iii) fuzzy set based approach and (iv) combined neural and fuzzy approach. Details of various LSZ mapping approaches can be found in Kanungo et al. (2006). In fact, the outputs generated in that study, i.e., various LSZ maps constitute the input of this study. Nevertheless, for the sake of completeness and continuity, a brief outline of these approaches for preparation of LSZ maps has been provided here.

A database of six thematic data layers pertaining to landslide causative factors namely lithology, slope, aspect, lineaments, land use land cover and drainage was created. These thematic data layers pertain to inherent factors representing ground characteristics of the terrain. Rainfall and earthquakes are external factors and are temporal phenomena and therefore were not considered in this study.

Remote sensing images from IRS-1C-LISS-III (acquired on 22nd March, 2000) and 1D-PAN (acquired on 3 April, 2000) sensors, Survey of India topographic

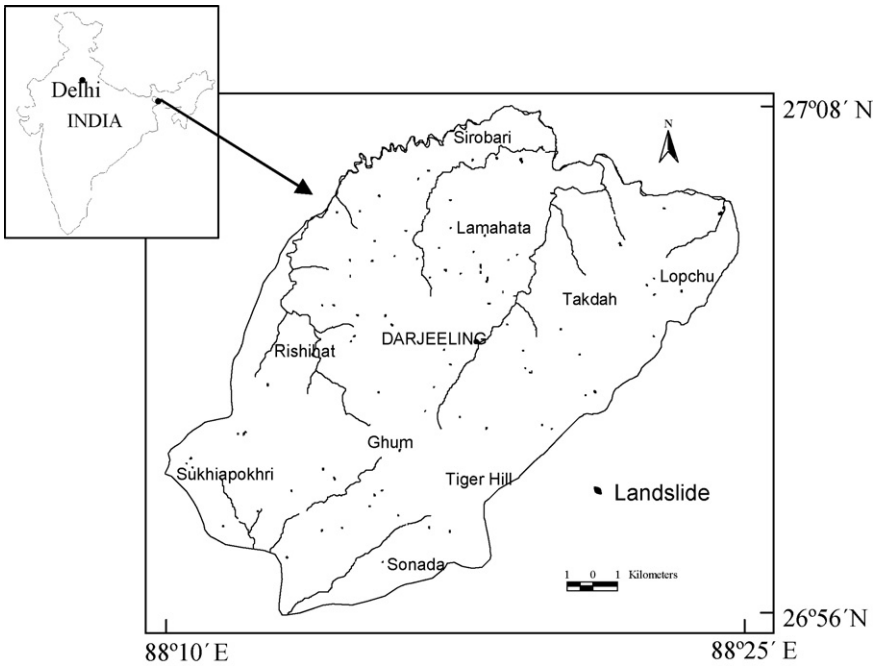

Fig. 1. Study area with landslide distribution in Darjeeling Himalayas.

maps at 1:25,000 and 1:50,000 scale, and the geological map at 1:250,000 scale published by Acharya (1989) formed the key data sources to generate the thematic data layers, which were rasterised at 25 m pixel size. Extensive field surveys were conducted during the years 2001–2003 to collect information on existing landslide distribution, which assisted in creation of training and testing data sets, finding out fuzzy membership values and for the validation and comparative evaluation of LSZ maps. A total of 101 landslides of varying dimensions (180–27,400 m^2) were mapped from remote sensing images and field surveys. Most of the observed landslides in the region were of rock slides type. However, in some cases, complex types of failure were also observed. The existing landslide distribution map was also converted to a rasterized thematic data layer at 25 m pixel size, which indicated that there were a total of 339 pixels that belonged to landslides in the region. The thematic database was input to four approaches to generate LSZ maps.

3.1. LSZ Map I using conventional weighting approach

The conventional weighting procedure involved assigning of weights and ratings to the thematic data layers and their categories respectively, based on the field knowledge of the area and the expert's (subjective) judgment. The weighted thematic data layers were generated by arithmetically multiplying the weight of the layer with the ratings of the corresponding categories of each layer. These layers were laid over one another and algebraically added to produce the LSZ map (referred here as Map I, Fig. 2a) representing five landslide susceptibility zones.

3.2. LSZ Map II using ANN black box approach

In this approach, the LSZ Map I obtained from conventional weighting approach was used as the reference map. Two independent training and testing datasets were created. Each dataset consisted of 2500 mutually exclusive pixels corresponding to 500 pixels per landslide susceptibility zone as identified from LSZ Map I. A total of 39 neural network architectures were designed and trained with Levenberg–Marquardt back-propagation algorithm. The adjusted connection weights obtained from the trained network were subsequently used to process the testing data to determine the generalization capability and the accuracy of the neural network. Finally, the adjusted connection weights obtained from an ANN with architecture 6/13/7/1 (6 neurons in input layer, 13 neurons in 1st hidden layer, 7 neurons in 2nd hidden layer and 1 neuron in output layer) producing the highest accuracy was subsequently used to determine

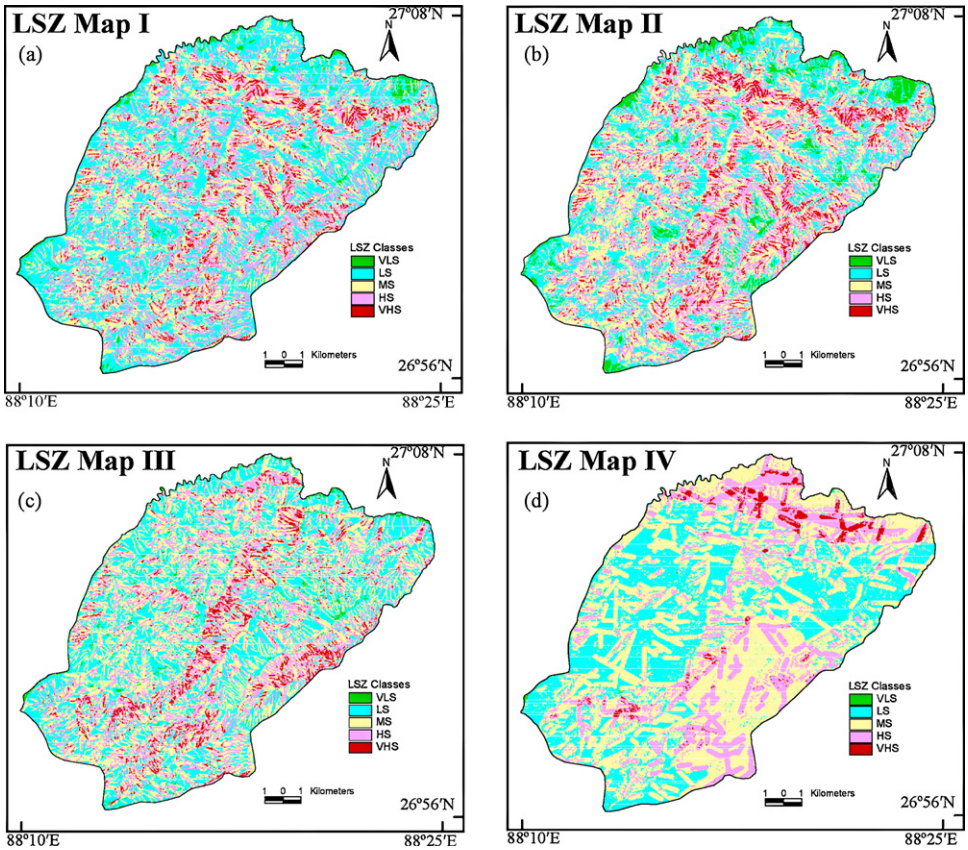

Fig. 2. LSZ maps using four different procedures. (a) Conventional weighting procedure. (b) ANN black box procedure. (c) Fuzzy set based procedure. (d) Combined neural and fuzzy procedure.

the network output of all the pixels in the study area and the LSZ map (referred here as Map II, Fig. 2b) was produced.

3.3. LSZ Map III using fuzzy set based approach

In this approach, ratings of each category of a given thematic data layer were determined using cosine amplitude similarity procedure (Ross, 1995; Ercanoglu and Gokceoglu, 2004). The landslide distribution map and different categories of thematic layers, taken one at a time, were considered as two datasets for the computation of ratings. These ratings were integrated in GIS to generate the LSZ map (referred here as Map III, Fig. 2c) by considering the weight of each thematic layer as unity.

3.4. LSZ Map IV using combined neural and fuzzy approach

The combined neural and fuzzy procedure involved three main steps: (i) weight determination of each thematic data layer through ANN connection-weight procedure, (ii) rating determination of categories of thematic layers using cosine amplitude similarity procedure, described in Section 3.3 and (iii) LSZ map preparation by integration of ratings and weights in GIS. A feed forward back-propagation multi-layer ANN with one input layer, two hidden layers and one output layer was considered. Three independent data sets were created for training, verification and testing. A total of 100 neural network architectures were designed, trained and tested with Levenberg–Marquardt back-propagation algorithm. The adjusted weights of input-hidden, hidden-hidden and hidden-output connections for each network were captured and simple matrix multiplication was performed on these weight matrices to obtain a 6×1 weight matrix for each network, which represented the weights of six causative factors. These causative factors were ranked according to the corresponding absolute weights for each network. The rank of a factor was decided based on the rank observed by the maximum number of networks (majority rule). Subsequently, the normalized average

of the weights of these networks at a scale of 0–10 was computed for a particular factor and assigned as the weight of that factor. The ratings of each category of thematic data layer were determined using fuzzy set based cosine amplitude method. The integration of 6 thematic layers representing the ratings for the categories of the layers and weights for the layers was performed using arithmetic overlay operation and the LSZ map (referred here as Map IV, Fig. 2d) was produced.

4. Comparative evaluation of LSZ maps

A comparative evaluation of four LSZ maps throws interesting light on their relative efficacy, differences and mutual compatibility. First a visual analysis of these maps is provided here.

Visual inspection of LSZ Map I revealed that all the five susceptibility zones were distributed all over the study area. The map thus did not show any well-defined pattern for the distribution of susceptibility zones. It was observed that the VHS and HS zones were represented mostly along 1st and 2nd order drainage buffer areas, which was mainly due to assignment of high weights and ratings subjectively to the categories of this causative factor. In the ANN black box procedure, the weights and ratings remained hidden and were not known. The LSZ Map II produced through this approach showed a lot of similarity with the LSZ Map I, because the latter map was used as the reference map to generate the LSZ Map II. Therefore, the outcome of this map was also biased towards conventional weighting procedure. The fuzzy set based procedure using cosine amplitude similarity approach could bring out the relative importance (ratings) of different categories of causative factors in terms of landslide occurrences in an unbiased manner. The LSZ Map III, produced from this approach, depicted an overall NNE-SSW landslide susceptibility zonation trend in the area. It was observed that the southeast and east facing slopes were more susceptible to landslides than other slopes, which led to the conclusion that there was a topographic control in this LSZ map. Further, an influence of drainage lines on landslide incidence and LSZ mapping was also observed. However, the major limitation of this approach was that all the factors were considered equally important as a unit weight was assigned to each factor. Alternatively, the map (LSZ Map IV) produced from combined neural and fuzzy procedure, wherein the weights to factors were assigned via neural network and ratings to categories via fuzzy set theory, revealed that lithology had the most significant effect whereas the drainage buffer had the least significant effect on landslide incidences in the area. The ANN derived weights also revealed the importance of lineaments. Thus, the LSZ Map IV reflected a preferential distribution of higher landslide susceptibility zones along structural discontinuities (lineaments), which should indeed be the case. Also, the Darjeeling gneiss rock type in south-eastern part, feldspathic greywacke and Reyang quartzite in the northern part of the study area indicated moderate to very high susceptibility zones.

This visual interpretation has now been substantiated with a quantitative comparative evaluation of the LSZ maps using three different approaches:

(a) Landslide density analysis.
(b) Error matrix analysis.
(c) Difference image analysis.

4.1. Landslide density analysis

Landslide density is defined as the ratio of the existing landslide area in percent to the area of each landslide susceptibility zone in percent, and is computed here on the basis of the number of pixels in the image. Landslide density values for each susceptibility zone for different LSZ maps have been computed separately (Table 1). Usually, an ideal LSZ map should have the highest landslide density for VHS zone, as compared to other zones and there ought to be a decreasing trend of landslide density values successively from VHS to VLS zone.

It is observed from Table 1 that the landslide densities for VHS zone of LSZ Maps III and IV are significantly higher than those obtained for other susceptibility zones. There is also a decreasing trend of landslide density values from VHS zone to VLS zone for Maps III and IV. On the other hand, the landslide density is found to be marginally higher for HS zone

Table 1
Landslide densities in landslide susceptibility zones of LSZ maps derived from conventional, ANN black box, fuzzy and combined neural and fuzzy approaches

Landslide susceptibility zones	Landslide density (computation based on pixel numbers)			
	LSZ Map I	LSZ Map II	LSZ Map III	LSZ Map IV
VHS	1.63	1.34	6.72	13.09
HS	1.79	1.50	1.11	1.58
MS	0.88	1.02	0.66	0.55
LS	0.41	0.49	0.26	0.40
VLS	0.19	0.12	0	0

than VHS zone in case of LSZ Maps I and II. It is also observed from Table 1 that the LSZ Maps I and II have a mutually similar trend of landslide densities for various susceptibility zones, which is on the expected lines, as the LSZ Map I has been used as the reference map to generate the LSZ Map II.

As far as the landslide density in VHS zone is concerned, it is observed that the LSZ Map IV has a markedly higher landslide density (>13) for this zone than that observed in other LSZ maps (1.63 for Map I, 1.34 for Map II and 6.72 for Map III). This may be due to more objectivity in the weight assignment process of the combined neural and fuzzy procedure. Further, Map IV also has a more systematic and reasonable trend of variation in landslide density values from VHS to VLS zones. Thus, based on the landslide density values of different landslide susceptibility zones and their trend from VHS to VLS zones for all the LSZ maps, it can be inferred that the combined neural and fuzzy procedure developed and implemented for LSZ mapping (LSZ Map IV) appears to be significantly better than other procedures (fuzzy, conventional and ANN black box procedures) used here, and the LSZ Map IV may be considered as the best LSZ map of the area (also see later Section 4.3).

4.2. Error matrix analysis

It is also important to investigate the match or mismatch of pixels across LSZ maps prepared based on different procedures. An error matrix analysis, proposed as a means of assessing the accuracy of land use land cover maps in the remote sensing literature (Congalton, 1991) can be utilized effectively to comparatively evaluate the LSZ maps.

Thus, in the present context, the error matrix is defined as the cross tabulation of distribution of pixels in various landslide susceptibility zones in a particular LSZ map and corresponding landslide susceptibility zones in another LSZ map. The error matrix analysis is based on cumulative number of pixels falling in each landslide susceptibility zone rather than on pixel-by-pixel basis. Here, three such error matrices have been generated to understand the distribution of number of pixels in various landslide susceptibility zones across the maps.

(a) Error matrix for LSZ Maps I and II.
(b) Error matrix for LSZ Maps III and IV.
(c) Error matrix for LSZ Maps I and IV.

The reasons for selecting only the above combinations are given under each evaluation.

Table 2
Error matrix of LSZ Maps I and II

	LSZ Map I					Total
	VHS	HS	MS	LS	VLS	
LSZ Map II						
VHS	23,703	7,306	94	10	0	31,113
HS	2,686	90,112	16,237	362	0	109,397
MS	43	11,448	98,700	33,831	5	144,027
LS	49	548	7,498	96,541	320	104,956
VLS	2	10	769	11,338	6,135	18,254
Total	26,483	109,424	123,298	142,082	6,460	407,747

4.2.1. Error matrix for LSZ Maps I and II

The LSZ Map I has been prepared through conventional weighting approach and it has been used as a reference map for generating LSZ Map II, based on the ANN black box approach. Therefore, for comparing the two maps, an error matrix generated between Map I and Map II is given in Table 2. It can be seen that there is a high degree of matching in the pixels of LSZ Maps I and II, particularly for VHS, HS, MS and LS zones, which is quite expected. However, there is some degree of mismatch in the VLS zone, which is reflected by the population of 6460 pixels in the VLS zone of LSZ Map I as against a population of 18,254 pixels in this zone in Map II.

4.2.2. Error matrix for LSZ Maps III and IV

The LSZ Maps III and IV have been prepared using two objective weighting procedures—the Map III based on fuzzy set based procedure and the Map IV based on combined neural and fuzzy procedure. Therefore, it is interesting to compare the two maps through error matrix (Table 3), which reveals that there is a general correspondence between these maps (Maps III and IV). About 50% pixels (201,634 pixels out of total 407,747 pixels), as indicated along the diagonal of the matrix, match in different zones. The VHS zone of

Table 3
Error matrix of LSZ Maps III and IV

	LSZ Map III					Total
	VHS	HS	MS	LS	VLS	
LSZ Map IV						
VHS	4,687	3,511	1,259	0	0	9,457
HS	15,219	32,495	31,922	2,766	0	82,402
MS	4,817	54,190	89,885	47,707	1,023	197,622
LS	17	2,392	37,466	73,475	3,692	117,042
VLS	0	2	20	110	1,092	1,224
Total	24,740	92,590	160,552	124,058	5,807	407,747

LSZ Map IV has a much focused population of 9457 pixels, whereas the LSZ Map III has a population of 24,740 pixels in the VHS zone. This is responsible for some mismatch in the VHS zone.

The analysis may also be related to the weight/rating procedures adopted for the preparation of the two maps. The weights for the factors are considered as constant (i.e., unit weight for all the factors) in case of fuzzy set based procedure and only ratings for the categories obtained from fuzzy set theoretic based procedure have been used for generating Map III. On the other hand, the ratings for the categories obtained from fuzzy set theoretic based procedure have been integrated with the weights for the factors (obtained from ANN connection weight procedure) to prepare the LSZ Map IV. Therefore, in case of combined neural and fuzzy procedure, the factors have varied importance in terms of weights. This may be responsible for differences in the two maps and mismatch between LSZ Maps III and IV.

4.2.3. Error matrix for LSZ Maps I and IV

The LSZ Map IV, prepared using fully objective combined neural and fuzzy procedure was found to be the best LSZ map. The map shows a much focused distribution of pixels in VHS zone. The LSZ Map I has been generated using the most widely used conventional weighting procedure. Therefore, a comparison of the two Maps I and IV has been carried out via error matrix (Table 4).

The first point to be noted is that in LSZ Map IV, there is an alarming difference in the number of pixels allocated to various landslide susceptibility zones. On the other hand, in case of LSZ Map I, the number of pixels is quite same in HS, MS and LS zones.

The error matrix shows that there is barely 37.8% match in number of pixels (154,055 pixels out of total 407,747 pixels) between the two maps. Thus, there is a lot of mismatch in number of pixels allocated to various zones in LSZ Maps I and IV. This mismatch may be due to the weight and rating assignment procedures of conventional weighting procedure (resulting into LSZ Map I) vis-à-vis combined neural and fuzzy procedure (resulting into LSZ Map IV). As the weights and ratings have been assigned in a purely subjective manner in case of conventional weighting procedure and in a purely objective manner in case of the combined neural and fuzzy procedure, the weights for the factors and the ratings for the categories significantly differ in both the procedures. This has resulted into two different LSZ maps (LSZ Maps I and IV), with high mismatch.

Table 4
Error matrix of LSZ Maps I and IV

	LSZ Map I					Total
	VHS	HS	MS	LS	VLS	
LSZ Map IV						
VHS	1,114	2,897	3,433	2,013	0	9,457
HS	11,583	25,584	27,478	17,150	607	82,402
MS	11,344	56,584	65,401	61,058	3,235	197,622
LS	2,442	24,340	26,952	61,323	1,985	117,042
VLS	0	19	34	538	633	1,224
Total	26,483	109,424	123,298	142,082	6,460	407,747

4.3. Difference image analysis

Difference image analysis elucidates how pixels shift from one landslide susceptibility zone to another zone, based on the LSZ mapping procedure adopted. Attributes 1, 2, 3, 4 and 5 have been assigned respectively to the VLS, LS, MS, HS and VHS zones of all the four LSZ maps. Difference images are generated by subtracting pixel attributes of one LSZ map from the other. Thus, a difference image can have a maximum five different classes; viz., no difference, one-zone difference, two-zone difference, three-zone difference and four-zone difference. Fully matching pixels in the two LSZ maps would correspond to the no difference class in the difference image. Thus, the difference image shows the spatial consistency between two LSZ maps in terms of matching/mismatching of pixels in various landslide susceptibility zones.

For this analysis, the same three different combinations of LSZ maps (i.e., Maps I and II, Maps III and IV and Maps I and IV) have been taken for comparative evaluation, as has been done for the error matrix analysis, the logic of selecting the combination remains the same. The results of difference image analysis are presented in terms of cumulative number of pixels and percent areas covered in each of the difference classes or zones (Table 5).

4.3.1. Difference image analysis of LSZ Maps I and II

The LSZ Map I, prepared using conventional weighting procedure, and Map II using the ANN black box procedure, appear quite alike, as can be observed from difference image of the two (Fig. 3a), which shows a high degree of mutual correspondence and matching of landslide susceptibility zones throughout the area. This is in agreement with the results based on error matrix analysis (Table 2). About 77.3% pixels have full mutual matching and 22.2% pixels exhibit one-zone difference. Barely 0.5% pixels have two-zone difference

Table 5
Results of difference image analyses of LSZ maps

Figure number	Difference images	No difference		One-zone difference		Two-zone difference		Three-zone difference		Four-zone difference	
		Number of pixels	Area (%)	Number of pixels	Area (%)	Number of pixels	Area (%)	Number of pixels	Area (%)	Number of pixels	Area (%)
3	I and II	315,191	77.3	90,664	22.2	1,821	0.5	69	0.0	2	0
4	III and IV	201,634	49.5	193,817	47.5	12,277	3.0	19	0.0	0	0
5	I–IV	154,055	37.8	189,075	46.4	59,536	14.6	5,081	1.2	0	0

(Fig. 3b) (and these appear to be related to a lithologic band in the northern part of the area). However, in general, there is a high degree of correspondence between LSZ Maps I and II.

4.3.2. *Difference image of LSZ Maps III and IV*

The LSZ Map III (Fig. 2c) (prepared using fuzzy set based procedure) and the LSZ Map IV (Fig. 2d) (prepared using combined neural and fuzzy procedure)

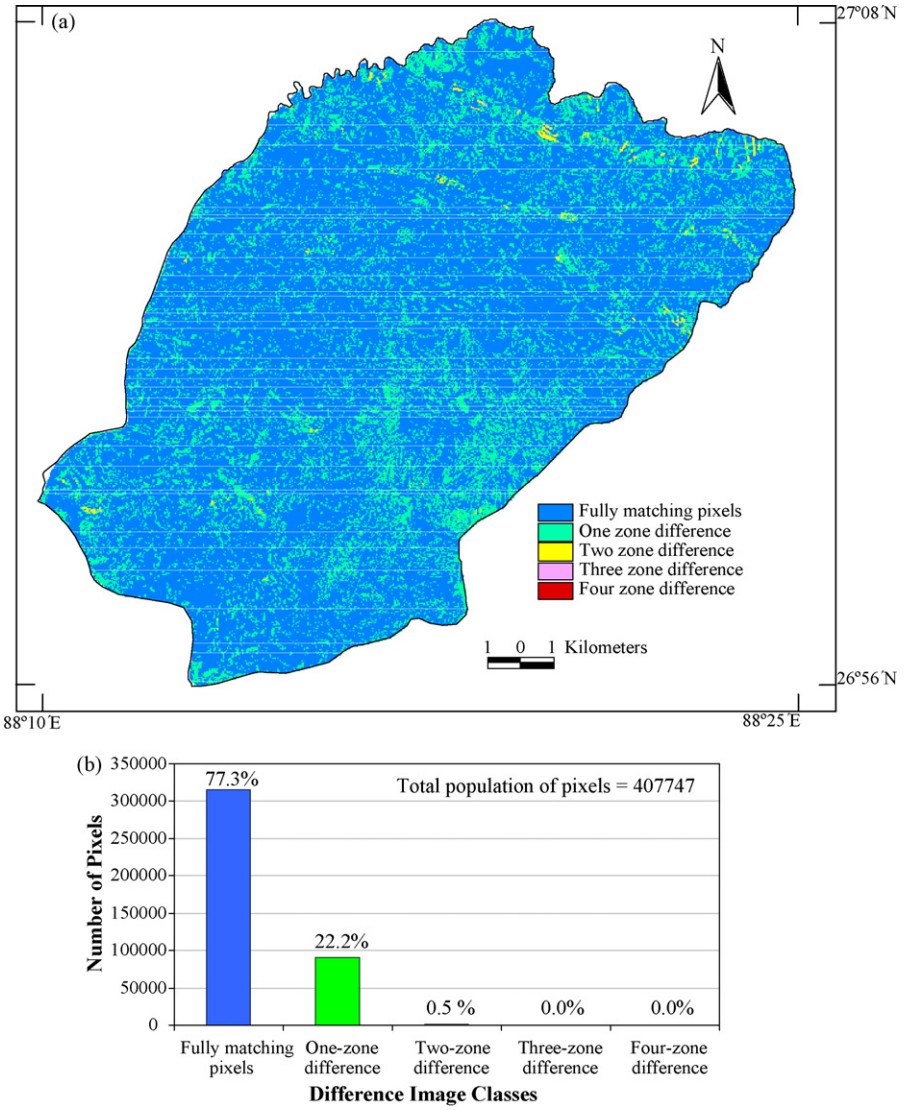

Fig. 3. (a) Difference image of LSZ Maps I and II. (b) Frequency distribution of pixels in difference image classes.

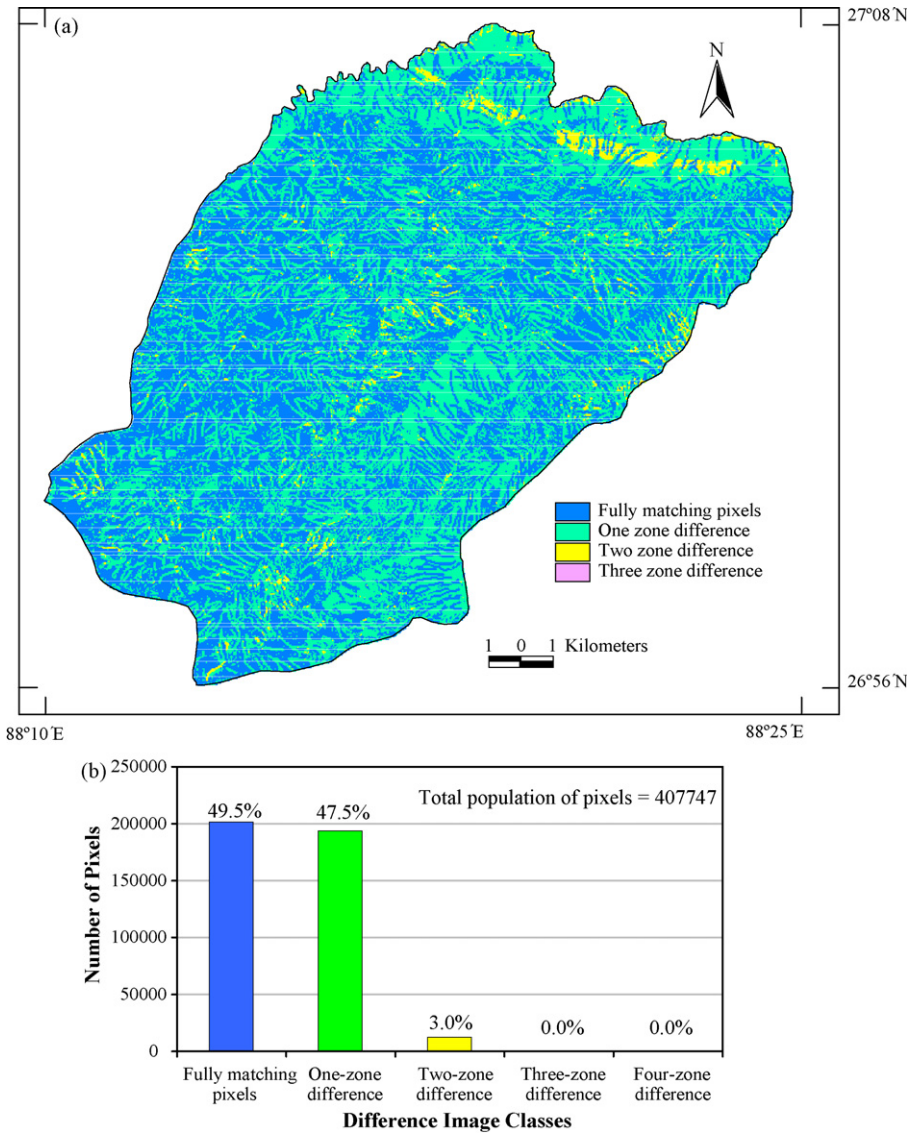

Fig. 4. (a) Difference image of LSZ Maps III and IV. (b) Frequency distribution of pixels in difference image classes.

have been generated based on objective weighting procedure. A difference image of the two (Fig. 4a) shows a high degree of spatial mutual correspondence. About 49.5% pixels have full mutual matching and 47.5% pixels exhibit only one-zone difference (Fig. 4b). Only about 3.0% pixels have two-zone difference. These broadly appear to be related to a lithologic band in the northern part of the area.

It may be recalled that in case of LSZ Map III, prepared using fuzzy set based procedure, all the causative factors have been given equal or unity weights and the importance of different categories of factors differ in terms of ratings. Ratings of categories vary between 0 and 1, within a causative factor (thematic layer). In case of LSZ Map IV, the ANN derived weights for factors are used and ratings are determined through fuzzy set based procedure. This has been done objectively without any bias. Therefore, the two LSZ maps differ slightly from each other.

In case of ANN derived weights, lithology has been assigned the highest weight of 4.8 (rank 1) whereas weights for other causative factors (lineament buffer, slope, aspect, land use land cover and drainage buffer) are found to vary from 2.1 to 0.2. As lithology has the highest and significantly higher weight than other factors in Map IV, the importance of lithology has been highlighted in the difference image analysis of Maps III and IV (Fig. 4a).

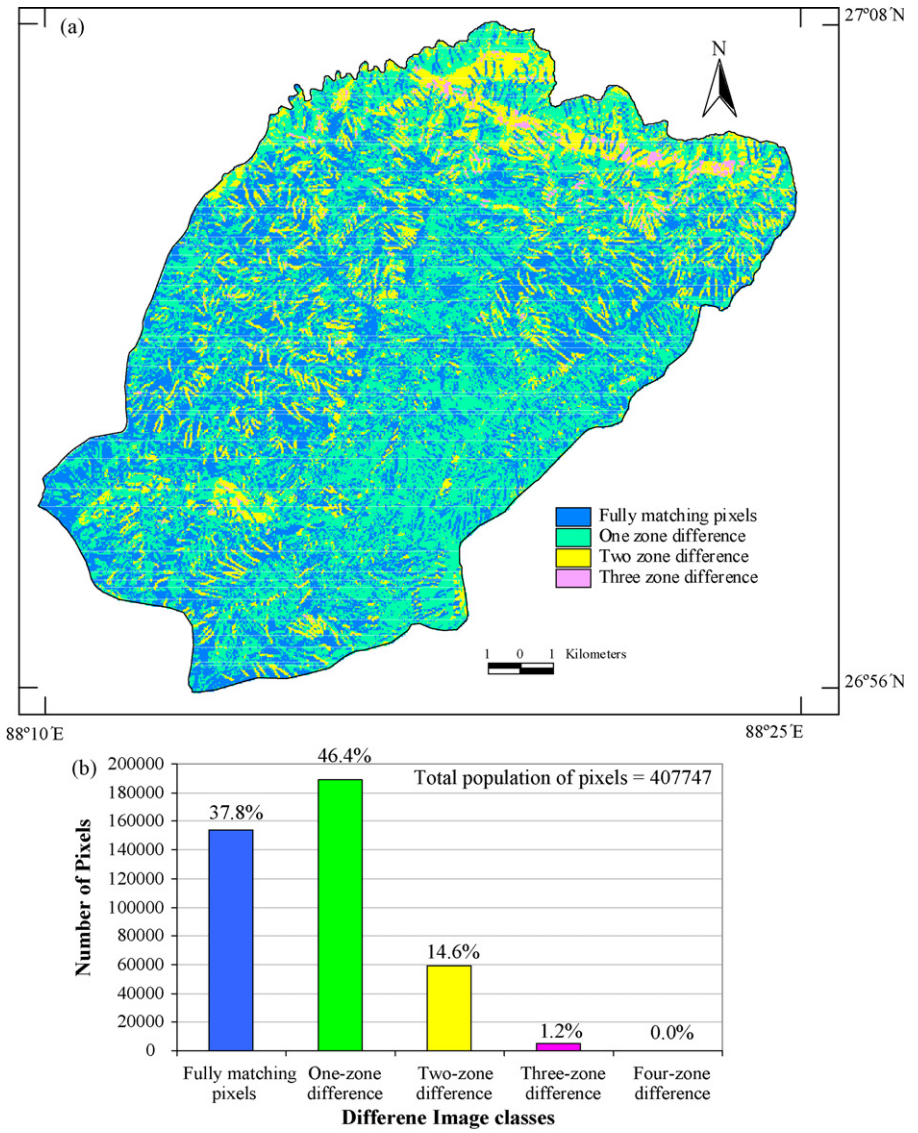

Fig. 5. (a) Difference image of LSZ Maps I and IV. (b) Frequency distribution of pixels in difference image classes.

Further, for LSZ Map IV, the ANN derived weights for lineament buffer, slope, aspect, land use land cover and drainage buffer are 2.1, 1.3, 1.1, 0.5 and 0.2, respectively. On the other hand, for LSZ Map III, all these weights have been considered as equal. Therefore, in difference image analysis of Maps III and IV, the impact of these factors has been found limited to fully matching and/or one-zone difference classes only (Fig. 4a).

4.3.3. Difference image of LSZ Maps I and IV

The LSZ Maps I and IV appear to exhibit the widest spatial difference, as was also seen through the error matrix analysis (Table 4). This fact is again corroborated in their difference image analysis (Fig. 5a), where only 37.8% pixels have been found to be fully matching, 46.4% pixels exhibit one-zone difference, 14.6% pixels have two-zone difference and 1.2% pixels have three-zone difference (Fig. 5b). This indicates a significant difference between the Maps I and IV.

A close look at the pattern of Maps I and IV reveals a wealth of interesting information. For preparing Map I, based on expert's opinions weights assigned to various thematic layers were: drainage buffer (weight = 9), lineament buffer (weight = 8), slope (weight = 7), lithology (weight = 6), land use land cover (weight = 4) and aspect (weight = 1). Therefore, the Map I (Fig. 2a)

shows significant impact of drainage lines/buffers and a little impact of lithology. On the other hand, the weights obtained from combined neural and fuzzy objective procedure (i.e., Map IV) were: lithology (weight = 4.8), lineament buffer (weight = 2.1), slope (weight = 1.3), aspect (weight = 1.1), land use land cover (weight = 0.5) and drainage buffer (weight = 0.2). Thus, this map distinctly exhibits the impact of lithologic banding and lineament buffer.

The difference image analysis of the two maps (Maps I and IV) clearly highlights the differences in the two maps. The most important is the band of two-zone difference lying in the northern part of the area, which apparently relates to lithology. Note that causative factor lithology has the highest rank (=1) in Map IV but a low importance (4th from top) in Map I. This difference in importance is responsible for the prominent band in the difference image in Fig. 5a.

Two-zone differences can also be seen at several places in the western and southern parts of the area (Fig. 5a). These are related to drainage buffer factor (highest importance in Map I and lowest importance in Map IV).

In the south-eastern part of Fig. 5a, most pixels exhibit no difference or only one-zone difference. This may be due to the superimposition/coincidence of lineament buffer vis-à-vis drainage buffer, i.e., the pixels being treated under drainage buffer in Map I, and under lineament buffer in Map IV. This is quite possible in situations where drainage lines follow lineaments, i.e., lineaments are marked by (rectilinear/rectangular/angular) drainage. In essence, lineaments lead to fracturing of the terrain along which development of drainage takes place. However, in the field due to limited field-of-view, drainage lines appear as a very conspicuous feature whereas lineaments are hardly observed. Considering the distribution of landslides in the field along the drainage lines, initially drainage line was considered to be the most important input thematic layer for LSZ, which led to generation of Map I. However, as a result of the objective spatial-domain regional analysis, drainage has been found to have the lowest rank (=6) in Map IV. Thus, the difference image analysis reveals that lineament has the most influence on the landslide occurrences whereas the drainage is only an apparent manifestation of the same at places.

5. Summary of results

In this study, the LSZ maps produced from different weight-rating procedures (viz. conventional, ANN black box, fuzzy and combined neural and fuzzy) were evaluated. The comparative evaluation was carried out using three approaches, landslide density distribution in various landslide susceptibility zones, error matrix analysis and difference image analysis. The results of the study have been summarised as:

(a) The LSZ Maps I (conventional) and II (ANN black box) are quite similar to each other. This is also expected as the Map I was used as the reference map for defining target outputs for the ANN procedure that resulted in Map II.
(b) The LSZ Maps III (fuzzy set based) and IV (combined neural and fuzzy based) exhibit similarity to each other in terms of landslide density values, error matrix and difference image analysis. This is because both the maps have been generated using objective weight assignment procedures.
(c) The LSZ Maps I and IV are found to depict the widest mutual spatial differences. This is again considered to be related to the manner in which the two maps were produced—Map I was based on highly subjective conventional weighting procedure and Map IV was derived from fully objective combined neural and fuzzy procedure.
(d) The LSZ Map IV (combined neural and fuzzy) is considered to be the best LSZ map of the area. This is because of the fact that it has a much higher landslide density value (>13) for VHS zone, as compared to other maps (1.63 for Map I, 1.34 for Map II, and 6.72 for Map III), and has a more systematic and reasonable trend of decreasing landslide density values from VHS through VLS zones.
(e) As far as the effects of various causative factors on the spatial patterns of LSZ Maps I, II, III, and IV are concerned, it is observed that each LSZ map genuinely reflects the relative weights of the input causative factor. For example, in the conventional weighting procedure, drainage buffer was given the highest weight, which was apparent in LSZ Map I as well as Map II. Further, in the combined neural and fuzzy procedure, the highest weight (4.8, rank 1) pertains to lithology, followed by lineament buffer (2.1, rank 2), and the effects of these input factors were also visible on LSZ Map IV.
(f) A difference image analysis of LSZ Maps I and IV is highly revealing. First, the importance of lithology, not so obvious from field data (LSZ Map I), was highlighted by the fully objectively derived LSZ Map IV. Further, it is seen that there is a superimposition/coincidence of lineament buffer vis-à-vis drainage buffer at places, i.e., the same

pixels are treated under drainage buffer in Map I and under lineament buffer in Map IV. This implies that drainage at places follows lineaments, i.e., lineaments have led to fracturing of the terrain along which drainage has developed. Although, in the field, drainage lines appear to control the distribution of landslides, the objective spatial domain regional analysis reveals that the lineament is the important factor.

6. Concluding remarks

The comparative analysis of LSZ raster maps shows the limitation of conventional weighting procedure, where weights are assigned based on field observations, which has its obvious limitations of limited perspective views (e.g. drainage being given highest weight, etc.). The fully objective procedure (combined neural and fuzzy) on the other hand could bring out in an unbiased manner the relative importance (weights) of causative factors (lithology and lineament). Therefore, the comparative evaluation of the maps using the three suggested approaches (i.e., landslide density analysis along with error matrix analysis and difference image analysis) elucidates the relative advantages of fully objective procedure vis-à-vis conventional weighting procedure for LSZ mapping. These approaches can thus be adopted for effective comparison of spatial maps produced from different procedures.

References

Acharya, S.K., 1989. The Daling Group, its nomenclature, tectonostratigraphy and structural grain: with notes on their possible equivalents. Geological Survey of Indonesia, Special Publication 22, 5–13.

Bonham-Carter, G.F., 1994. Geographic Information Systems for Geoscientists: Modelling with GIS. Pergamon, Ottawa, p. 398.

Carrara, A., Guzzetti, F. (Eds.), 1995. Geographical Information Systems in Assessing Natural Hazards. Academic Publisher, Kluwer, Dordrecht, The Netherlands, p. 353.

Congalton, R.G., 1991. A review of assessing the accuracy of classifications of remotely sensed data. Remote Sensing of Environment 37, 35–46.

DeMers, M.N., 2000. Fundamentals of Geographic Information Systems, second ed. John Wiley & Sons, New York, p. 498.

Ercanoglu, M., Gokceoglu, C., 2004. Use of fuzzy relations to produce landslide susceptibility map of a landslide prone area (West Black Sea Region, Turkey). Engineering Geology 75 (3 and 4), 229–250.

Gonzalez, R.C., Woods, R.E., 2002. Digital Image Processing, second ed. Prentice Hall, New Jersey, p. 779.

Gupta, R.P., 2003. Remote Sensing Geology, second ed. Springer-Verlag, Berlin, Heidelberg, Germany, p. 655.

Gupta, R.P., Joshi, B.C., 1990. Landslide hazard zonation using the GIS approach—a case study from the Ramganga Catchment, Himalayas. Engineering Geology 28, 119–131.

Gupta, R.P., Saha, A.K., Arora, M.K., Kumar, A., 1999. Landslide hazard zonation in a part of Bhagirathy Valley, Garhwal Himalayas, using integrated remote sensing—GIS. Journal of Himalayan Geology 20 (2), 71–85.

Hagen, A., 2003. Fuzzy set approach to assessing similarity of categorical maps. International Journal of Geographical Information Science 17 (3), 235–249.

Kanungo, D.P., Arora, M.K., Sarkar, S., Gupta, R.P., 2006. A comparative study of conventional, ANN black box, fuzzy and combined neural and fuzzy weighting procedures for landslide susceptibility zonation in Darjeeling Himalayas. Engineering Geology 85, 347–366.

Monserud, R.A., Leemans, R., 1992. Comparing global vegetation maps with the Kappa statistic. Ecological Modelling 62, 275–293.

Pontius Jr., R.G., Huffaker, D., Denman, K., 2004. Useful techniques of validation for spatially explicit land-change models. Ecological Modelling 179 (4), 445–461.

Ross, T.J., 1995. Fuzzy Logic with Engineering Applications. McGraw-Hill, New York.

Saha, A.K., Gupta, R.P., Sarkar, I., Arora, M.K., Csaplovics, E., 2005. An approach for GIS-based statistical landslide susceptibility zonation—with a case study in the Himalayas. Landslides 2, 61–69.

Sarkar, S., Kanungo, D.P., 2004. An integrated approach for landslide susceptibility mapping using remote sensing and GIS. Photogrammetric Engineering and Remote Sensing 70 (5), 617–625.

Sarkar, S., Kanungo, D.P., Mehrotra, G.S., 1995. Landslide hazard zonation: a case study in Garhwal Himalaya, India. Mountain Research and Development 15 (4), 301–309.

Winter, S., 2000. Location similarity of regions. Photogrammetric Engineering and Remote Sensing 55 (3), 189–200.